

Communication

Assessing Bioremediation of Soils Polluted with Fuel Oil 6 by Means of Diffuse Reflectance Spectroscopy

Víctor J. García ^{1,2,*}, Carmen O. Márquez ^{3,4}, Andrés R. Cedeño ³ and Kleber G. Montesdeoca ³

¹ Facultad de Ingeniería, Escuela de Ingeniería Civil, Universidad Nacional de Chimborazo, Riobamba, Provincia de Chimborazo 060150, Ecuador

² Facultad de Ciencias, Universidad de Los Andes, Mérida, Estado Mérida 5101, Venezuela

³ Facultad de Ingeniería, Escuela de Ingeniería Ambiental, Universidad Nacional de Chimborazo, Riobamba, Provincia de Chimborazo 060150, Ecuador; cmarquez@unach.edu.ec (C.O.M.); andres_acs91@hotmail.com (A.R.C.); kleermontesdeoca@gmail.com (K.G.M.)

⁴ Facultad de Ciencias Forestales y Ambientales, Universidad de Los Andes, Mérida, Estado Mérida 5101, Venezuela

* Correspondence: vgarcia@unach.edu.ec

Received: 20 November 2018; Accepted: 8 February 2019; Published: 13 February 2019



Abstract: This study aimed to assess the bioremediation of soils polluted with fuel oil 6 (FO6) using diffuse reflectance (DR) spectroscopy in the visible and near infrared (Vis-NIR) electromagnetic spectrum. To achieve our goal, we determined the spectral signature of fuel oil 6 (FO6), developed a calibration model to quantify the total petroleum hydrocarbons (TPH), and assessed the bioremediation in soils contaminated with FO6 and inoculated with *Pseudomonas aeruginosa*. Surface soil samples (SS) (0–30 cm depth) from uncontaminated Entisol soil from Termoesmeraldas Thermal Power Plant, Ecuador and quart sand (QS) samples were spiked with FO6 at a known contamination of 0.5, 1, 3, 6, 9, 12 wt.% on a gravimetric basis. A sample of contaminated Entisol soil was taken to isolate *P. aeruginosa* from a spill site located in Termoesmeraldas. *P. aeruginosa* was successfully augmented in a molasses medium. The results suggested that the C–H stretch combination overtone band around 2300 nm is the one that makes the significant contribution to the FO6 spectral signature and for the analysis of FO6 contaminated Entisols soil. The calibration model for QS samples and SS showed an excellent agreement with experimental data $R^2 = 0.9989$ and $R^2 = 0.9968$, respectively. The TPH at 0, 7, 14, 21, and 23 days after inoculation were found using a calibration model developed and the Unach hydrocarbon index (UHI). While the QS samples showed the lower recovery rate (13.6%), the Entisols SS showed the higher recovery rate (45.8%) in 23 days. The use of DR spectroscopy and determination of the FO6 spectral signature allowed the assessment of the bioremediation process of QS and Entisols SS samples. The results showed that DR decreased with increasing the FO6 concentration and soil properties affected the degree of biodegradation.

Keywords: fuel oil 6; spectral signature; entisols soil; soil bioremediation; hydrocarbon index; total petroleum hydrocarbons

1. Introduction

Fuel oil 6 (FO6) is the heaviest commercial fuel that can be obtained and is one of the primary sources of energy in the production of electricity in several countries. Fuel oil 6 is the leading petroleum product present in leaks and spills, especially in the contamination of soil resource during production, transport, storage, and utilization. Soil contamination with FO6 has global dimensions and a significant impact on the long-term functioning of the soil ecosystem (water infiltration, percolation and retention, gas exchanges, soil organic matter and mineral nutrients dynamics, soil microbial biomass, diversity

and activity, and the susceptibility of soil to erosion). There is a considerable gap in the understanding of the impact of soil contamination with FO6 and the long-term recovery of soil functionalities, as well as on the resilience of the soil ecosystem. There is a need to develop technologies and a soil remediation technique to reduce the environmental footprint and set a platform for land reuse [1]. In this framework, bioremediation approaches have the potential to remediate sites while enhancing soil properties that support soil microbiota and plant communities. Bioremediation is the use of microorganisms and other soil inhabitants owing to their diverse metabolic capabilities to degrade, remove or otherwise control contaminants [2] and is believed to be non-invasive, and its cost is less than that of traditional techniques [3]. Bacteria are the most active agents in petroleum biodegradation. Nearly a hundred species of bacteria, representing thirty microbial genera, have been found to degrade petroleum products [4–6]. One of the most consistently isolated hydrocarbon-degrading bacteria from soil is *Pseudomonas* [7]. *Pseudomonas aeruginosa* produces rhamnolipids, a biosurfactant useful in the removal of oils and related products [8].

The overtone (harmonics) of fundamental modes of vibration of FO6 hydrocarbons enables its identification through portable instruments or remote sensing processes based on the diffuse reflectance (DR) spectrum (through its spectral signature). Scafutto et al. [9] measured and assembled in a spectral library the DR spectra of several mineral substrates impregnated with crude oils (API 19.2, 27.5, and 43.2), diesel, gasoline, and ethanol. Scafutto et al. [9] showed the potential of DR spectroscopy identifying contaminant density and the level of impregnation in soils mixtures using close- and far-range remote sensing techniques. Chakraborty et al. [10] studied the effects of soil type and organic carbon on VisNIR reflectance spectra of two contaminated soils. Chakraborty et al. [10] concluded that DR spectroscopy is a promising tool that would enable soil and environmental scientists to characterize contaminated soils at a much larger scale and for larger geographic areas. Douglas et al. [11] demonstrated that partial least-regression analysis with full cross-validation of spectral reflectance data estimates the amount of polycyclic aromatic hydrocarbons in petroleum-contaminated tropical rainforest soils to inform risk assessment and remediation. Okparanma et al. [12,13] used DR spectroscopy to develop soil maps of polycyclic aromatic hydrocarbons, and they concluded that the Vis-NIR DR spectroscopy approach might be useful for monitoring hydrocarbon contamination in a petroleum release site. Douglas et al. [14] concluded that Vis-NIR spectroscopy coupled with a random forest artificial intelligent algorithm offers an effective method for rapid quantification of total petroleum hydrocarbons (TPH) in soils. Schwartz et al. [15] concluded that DR spectroscopy could be used as a viable, rapid, cost-effective, environmentally friendly tool to determine TPH in five contaminated soils (Tipic xerofluvent, Tipic xerochrept, Tipic Chromoxerert, Lithic ruptic xerochrept, and Lithic haploxeroll) spiked with a known concentration of 95 octane fuel, diesel, and kerosene. However, in our knowledge, there are no studies of Entisols soil spiked with heavy crude oil (FO6 API 11.5°). Moreover, there are no studies that couple DR spectroscopy and FO6, despite the energetic relevance of FO6 and the frequent FO6 spill.

The Federal Institute of Geosciences and Natural Resources of Germany showed that airborne hyperspectral remote sensing could be used to detect hydrocarbons [16]. Hydrocarbons have typical characteristics that become visible in the DR spectrum [16]. Two hydrocarbon quantity indicators based on DR spectroscopy have been proposed to map petroleum hydrocarbons in soil: (1) The hydrocarbon index proposed by Kühn et al. [17] and Smejkalová et al. [18] and (2) the hydrocarbon index proposed by National Aeronautics and Space Administration (NASA) [18–20]. Both studies yielded limited results [13]. More recently, García et al. [21] developed a methodology that allows to quantify the hydrocarbons in the soil using DR spectroscopy. This study aimed to assess the bioremediation of soils polluted with FO6 by means of DR spectroscopy in the Vis-NIR electromagnetic spectrum. To achieve our goal, we determined the spectral signature of fuel oil 6 (FO6), developed a calibration model to quantify the total petroleum hydrocarbons (TPH), and assessed the bioremediation in soils contaminated with FO6 and inoculated with *P. aeruginosa*.

2. Materials and Methods

2.1. The Study Area, Soil Sampling, and Pretreatment

Pristine soil samples (SS) were collected from three selected uncontaminated sites from the lands of Termoesmeraldas Thermal Power Plant, Ecuador (0°57'33" N and 79°39'14" W). Termoesmeralda is located in a coastal area to 18 mamsl in the Esmeraldas Province. The predominant soils in the study site are derived from the alluvial plain, which has been formed as a result of the flooding of the Esmeraldas River, and its texture is silty-loam (clay (10%), silt (52%), and sand (38%)). According to the United States Department of Agriculture (USDA) soil taxonomic order, the soil sampled belongs to the order Entisols, suborder Fluvents, and the Ustifluvents group. Typical reported means of soil nutrients concentrations are 926.64 mg N/kg, 148.5 mg P/L, 2175 mg K/L, 3100 mg Mg/L, and 11,500 mg Ca/L. The mean pH and total organic carbon value are 7.2 and 1.35%, respectively.

Surface soil samples (0–30 cm depth) were collected by first removing the organic materials such as crop residues and grasses from the surface. We collected 5 kg of soil in each site, and then the three samples were mixed and homogenized to have 15 kg of noncontaminated bulk soil. The soil sample was stored in a polythene zipper bag and transported to the laboratory for soil processing and analysis. Before use, soil subsamples were sifted through a 2 mm sieve and sterilized in an autoclave for 4 h and at 115 °C.

One group of 18 soil samples (SS) were spiked with FO6 at a known contamination of 0.5, 1, 3, 6, 9, and 12 wt.% on a gravimetric basis. Based on these 18 samples (three samples for each concentration), a calibration model was developed. Additional, 3 soil samples were spiked with FO6 at a concentration of 6 wt.% on a gravimetric basis and for the monitoring bioremediation experiment.

A sample of contaminated soil was taken to isolate *P. aeruginosa* from a spill site located in Termoesmeraldas. We collected the soil sample using the directed sampling method from a 15 cm depth in plastic containers and preserved until shipment.

2.2. Quartz Sand Sampling and Pretreatment

Quartz sand (QS) (Arenas®Colma Fina provided by Sika Ecuatoriana S.A. (Quito, Pichincha, Ecuador)) sized from 400 to 74 µm was used for the FO6 spectral signature determination, calibration model development, and monitoring the bioremediation experiment.

One group of 18 QS samples were spiked with FO6 at a known contamination of 0.5, 1, 3, 6, 9, and 12 wt.% on a gravimetric basis. Based on these 18 samples (three samples for each concentration), a calibration model was developed, and the spectral signature of QS was determined. Additional, 3 QS samples were spiked with FO6 at a concentration of 6 wt.% for the monitoring bioremediation experiment.

2.3. Fuel Oil 6

The FO6 provided by Termoesmeraldas Thermal Power Plant is the residue that remains after the distillation of crude oil to obtain gasoline, naphtha, and diesel. Consequently, the FO6 composition is more complicated than other petroleum products, and its impurity content is higher. Table 1 lists the physicochemical characteristics of the FO6. The carbon range (number of carbon atoms) within FO6 varies from C20 to C40 (alkenes), and approximately 25% are polycyclic aromatic hydrocarbons (PAHs), 15% paraffinic, 45% naphthenic, and 15% of compounds containing metals, oxygen or sulfur. The PAHs are dangerous and persistent FO6 compounds that can put people's health at risk and cause harm to the environment. Alkenes, in general, have toxic, carcinogenic, and mutagenic properties and represent a significant danger to health and the environment [6].

Table 1. The physicochemical characteristics of fuel oil 6.

Property	Value
Gravity API, @ 60 °F *	11.5°
Kinematic Viscosity @ 50 °C *	628.4 cSt
Water and sediment *	0.05 vol.%
Ashes *	0.056 wt.%
Conradson coal waste *	15.5 wt.%
Asphaltenes	12.8 wt.%
Vanadium *	242 ppm
Sodium *	17 ppm
Nickel *	79 ppm
Sulfur *	1.96 wt.%
Paraffins **	5.9 vol.%
Alkylbenzenes **	1.9 vol.%
Naphthalenes **	2.6 vol.%
Phenanthrenes **	11.6 vol.%
Other Aromatic Hydrocarbons **	57.8 vol.%

References [21] * and [22] **.

2.4. *Pseudomonas Aeruginosa* Isolation and Identification

1. *Growth medium*: Twelve Petri plates that have a thin layer of agar-based growth medium—Difco™ Cetrinide agar base (Becton, Dickinson and Company, Franklin Lakes, NJ, USA) were prepared by spreading 15 to 20 mL of agar-base on the plate's bottom.
2. *Inoculation of the growth medium*: One gram of contaminated soil was mixed with 9 mL of sodium salt solution (NaCl 1%) to obtain a 10^{-1} dilution, and it was vortex shaken for 1 min. The contaminated soil was diluted to 10^{-2} , 10^{-3} , 10^{-4} , 10^{-5} , and 10^{-6} . One milliliter of each dilution was spread in a Petri plate to obtain six plates with an inoculated growth medium. Then, inoculated agar plates were incubated for 24 h at 36 °C.
3. *Identification*: The identification of the bacterial strain was carried out by applying the API-20e kit (bioMérieux Inc., Hazelwood, MO, USA), which serves to identify a different genus of bacteria and gram-negative bacilli. This kit works through 20 microcapsules containing different dehydrated reagents. These reagents, when coming into contact with the bacteria, produce a reaction that generates a specific coloration of the bacteria under study. It is considered a positive reaction in those where a color change has occurred. Based on the colors generated by each reaction and the numbering system for tests with positive results, a numerical code is obtained. The code was used as input in a macro found on page <http://www.biomerieux-usa.com/clinical/api>. The results of this macro confirmed that the combination of colors obtained corresponded 99.7% to *P. aeruginosa*.

2.5. Bioaugmentation

1. All the remains in each inoculated agar plate were placed in 1 liter of molasses (Brix grade 85) at 6 wt.%, and we left them in incubation 24 h at 35 °C.
2. One milliliter of culture (molasses and *P. aeruginosa*) was mixed with 9 mL of distilled water to obtain a 10^{-1} dilution in a tube. Similarly, we prepared dilutions at 10^{-2} , 10^{-3} , 10^{-4} , 10^{-5} , and 10^{-6} .
3. One milliliter of each dilution was spread in an agar-based growth medium to obtain six plates with an inoculated growth medium. Then, inoculated agar-based growth medium plates were incubated in an inverted position (agar side up) at 36 °C for 24 h.
4. Total cell count was determined before and after bioaugmentation. The counting method was counting chamber (hemocytometer). Thus, bioaugmentation was verified from the difference between the number of colonies forming units (CFU) prior to inoculation (433×10^4 CFU (Plate 3)

and 68×10^5 CFU (Plate 4) given as average 5.57×10^6 CFU) and the number of CFU after the bioaugmentation process: 1031×10^6 CFU. Given the initial volume of the dilution, it is considered that the dilution concentration is 1031×10^6 CFU/mL.

2.6. Inoculation of FO6 Contaminated Samples

Before leaving in incubation the 1 litre of molasses with the remains of the inoculated agar plate (see paragraph 1, Section 2.4), we took 20 mL of culture solution and spread in 200 g of FO6 contaminated sample. A glass stir stick was used to homogenize the mixture. We spiked with FO6 21 SS and 21 QS samples.

Upon the inoculation of the contaminated samples, we record the DR spectra of the 21 SS and 21 QS samples used for the development of a calibration model and assessing the bioremediation experiment. For the bioremediation experiment, the recorded DR spectrum count as the spectrum on day 0 (D0), the contaminated samples were left in incubation at 36 °C. The contaminated samples were taken out and returned to the incubation environment on day 7, 14, 21, and 23, with the purpose of registering their DR spectrum.

2.7. Measurement of Reflectance Spectra

The DR spectra of samples were measured in a proximal mode over the VisNIR region (350–2500 nm) using a portable spectroradiometer (Fieldspec®4 radiometer, Analytical Spectral Devices Inc., Boulder, CO, USA) and a halogen–quartz–tungsten lamp as a light source. About 200 g of each sample was placed near the instrument detector in a black holder of high-density polyethylene (10 cm diameter), and the surface was gently levelled with a metal spatula. The DR spectrum was recorded by illuminating the sample with a 75 W Lowel Pro-Light lamp at a 45°. The optic of the radiometer was vertically aligned with the axis passing through the geometric center of the samples, and its height was adjusted in such a way that only light reflected from the surface of the materials filled the field of view of the instrument. The detector distance to the surface of the samples was 30 cm. A spectralon panel (Labsphere Inc., North Sutton, NH, USA) with 99% reflectance was used to optimize and white-reference the spectroradiometer.

The internal configuration of the spectroradiometer consists of three detectors, each collecting spectra from three different spectral regions: 350–1000 nm, 1000–1800 nm, and 1800–2500 nm. The spectra collected by these detectors were not spliced, so each spectrum was corrected, splicing the three aforementioned spectral regions and using the ASD ViewSpec Pro™ software (ASD Inc., Boulder, CO, USA). Spectra were recorded consecutively in different angular orientations to eliminate undesirable effects in the spectrum. DR spectra were recorded when the sample was in each of the following angular positions: 0, 90, 180, and 270 degrees. These angles correspond to the angle that sustains the line that divides the sample into two halves, with the vertical plane that contains the light source and the detector. In its initial position, this angle is zero, which means that the line segment that divides the sample in two is in the reference plane. Once the spectra were registered in this position, the sample was rotated 90 degrees in the clockwise direction, and new spectra were recorded. This process continued until the total rotation angle was 270 degrees. In each of these angular positions, 10 spectra were recorded consecutively and repeatedly. Thus, 40 spectra were recorded for each sample. Spectral reflectance data for each sample were generated by arithmetic averaging of four replicated measurements (40 spectra) for that sample. Table 2 shows the total number of the registered spectrum.

Table 2. The total number of diffuse reflectance spectra recorded.

Angular Position	Spectra Recorded	Spectra Per Sample	Samples	Spectra Per Day	Monitoring Days	Total Spectra
Spectral signature and calibration model						
0°	10					
90°	10					
180°	10					
270°	10	40	6 × 3 × 2	40 × 36 = 1440	1	1 × 1440 = 1440
Bioremediation						
0°	10					
90°	10					
180°	10					
270°	10	40	3 × 2	40 × 6 = 240	5	5 × 240 = 1200

2.8. Fuel Oil 6 Spectral Signature

The combination of overtones of vibrational modes of C–O, C–H, N–H, and OH characterize the DR spectrum of FO6. The elucidation of the spectral signature of the sample from the DR spectrum is not a straightforward task. Therefore, we visually compared the DR spectrum of the pristine sample and contaminated sample, and the first derivative of the DR spectra of the pristine sample and the first derivative of the DR spectrum of the contaminated sample. We used the Savitzky–Golay algorithm (second order polynomial and window of 10 wavelengths), implemented in the Origin Lab 9.1 platform (<http://www.originlab.com>) for the calculation of the first derivative of the DR spectra. The first derivative of the DR spectra makes it possible to more easily visualize the aspects of the DR spectrum that are exclusively due to the FO6, achieving the identification of DR spectrum regions that are mainly due to the presence of FO6.

2.9. Determination of the Total Petroleum Hydrocarbon Using the Unach Hydrocarbon Index

The Unach hydrocarbon index (*UHI*) and the total petroleum hydrocarbons (*TPH*) were calculated following the procedure reported by García et al. [20]. The *UHI* and *TPH* values were calculated using the equations in row 4 in Table 3 and Equation (1), respectively.

$$TPH = \sum_{i=0}^n a_{i+1}(UHI)^i \quad (1)$$

In Equation (1), *n* represents the degree of the polynomial function, and it represents a generic value of the set of values of the polynomial function coefficients, which result from fitting the experimental data to a polynomial function; *a_{i+1}* represents a generic value of the set of values of the polynomial function coefficients, which result from adjusting the experimental data to a polynomial function. The polynomial function works as a calibration model for further quantification, and it is one for each material being studied. For the sake of clarity, we show in Table 3 a resume of hydrocarbons indicators based on DR spectroscopy and proposed by Kühn et al. [17], Smejkalová et al. [18], NASA [5,18,19], and García et al. [20].

Table 3. Hydrocarbon quantity indicators based on diffuse reflectance spectroscopy.

Indicators	
$KHI = \frac{\lambda_1 - \lambda_2}{\lambda_3 - \lambda_1} (\rho_3 - \rho_1) + (\rho_1 - \rho_2)$ [17,18]	$\rho_1, \rho_2,$ and ρ_3 are the measured values of the reflectance at the wavelength $\lambda_1 = 1705$ nm, $\lambda_2 = 1729$ nm, and $\lambda_3 = 1741$ nm, respectively.
$NHI = \frac{\rho_1 + \rho_3}{2 \times \rho_2}$ [5,18,19]	$\rho_1, \rho_2,$ and ρ_3 are the measured values of the reflectance at the wavelength $\lambda_1 = 2297$ nm, $\lambda_2 = 2313$ nm, and $\lambda_3 = 2329$ nm, respectively.
$UHI = a + b \frac{R_1}{\bar{R}} + c \frac{R_2}{\bar{R}} + d \frac{R_3}{\bar{R}}$ [20]	$R_1 = \left[\frac{\rho_{2230} + \rho_{2231} + \dots + \rho_{2230+m}}{1+m} \right]; R_2 = \left[\frac{\rho_{2285} + \rho_{2286} + \dots + \rho_{2285+m}}{1+m} \right];$ $R_3 = \left[\frac{\rho_{2314} + \rho_{2315} + \dots + \rho_{2314+m}}{1+m} \right]; \bar{R} = \frac{R_1 + R_2 + R_3}{3}.$ <p>The “rho” character represents the measured value of reflectance; the subscripts represent the range of wavelengths expressed in nanometers; m, represents the width of the range of wavelengths, and it is expressed in multiples of units of nanometers. Letters “a”, “b”, “c”, and “d” are constants.</p>

Finally, we developed a calibration model for estimating the total petroleum hydrocarbon from the DR spectrum of the sample under bioremediation. We used a one-way ANOVA and $p = 0.05$ followed by a Tukey’s HSD (Honestly significant difference) test to evaluate if there was a statistically significant difference in the *TPH* values. The Minitab 2009 (Minitab Inc., State College, PA, USA) was used for the statistical analysis of the data.

3. Results and Discussion

3.1. Fuel Oil 6 Spectral Signature

The FO6 spectral signature in the QS sample was appreciated around 2270 nm (Figure 1). Although the FO6 concentration was 0.5% on gravimetric bases, it was possible to elucidate the FO6 spectral signature. This result agrees with Cloutis’s [23] conclusion that potential spectral bands for hydrocarbon overtones are around 1700 nm and between 2200 and 2300 nm in the DR spectrum. Cloutis [23] reported the DR spectrum of medium-bitumen tar sand and observed hydrocarbons combined vibrational fundamental mode around 2300 nm. Similarly, Hörig et al. [16], while studying the potential detection of petroleum hydrocarbons by the airborne hyperspectral remote sensing, reported spectral features in the DR spectrum around 1730 nm and 2300 nm [24]. More recently, Scafutto et al. [9] reported that absorption bands exhibited by crude oil and fuels are attributed to primary overtone combination of C–H stretching modes of saturated CH_2 and terminal CH_3 , or aromatic C–H functional groups [9].

The first derivative of the DR spectra exhibits a spectral feature around 2270 nm due to FO6 (Figure 1b). A similar spectral feature was presented in the DR spectrum of the sample spike with FO6 (Figure 1b), while it was not present in the DR spectra of the uncontaminated sample (Figure 1a). The absorption band around 2300 nm can be attributed to FO6 spectral signatures (stretch + bend) and therefore linked to petroleum hydrocarbons [11,14]. Therefore, we used the absorption bands of hydrocarbons around 2300 nm to identify uncontaminated from contaminated samples and to develop a calibration model to quantify the *TPH* in FO6 contaminated soils.

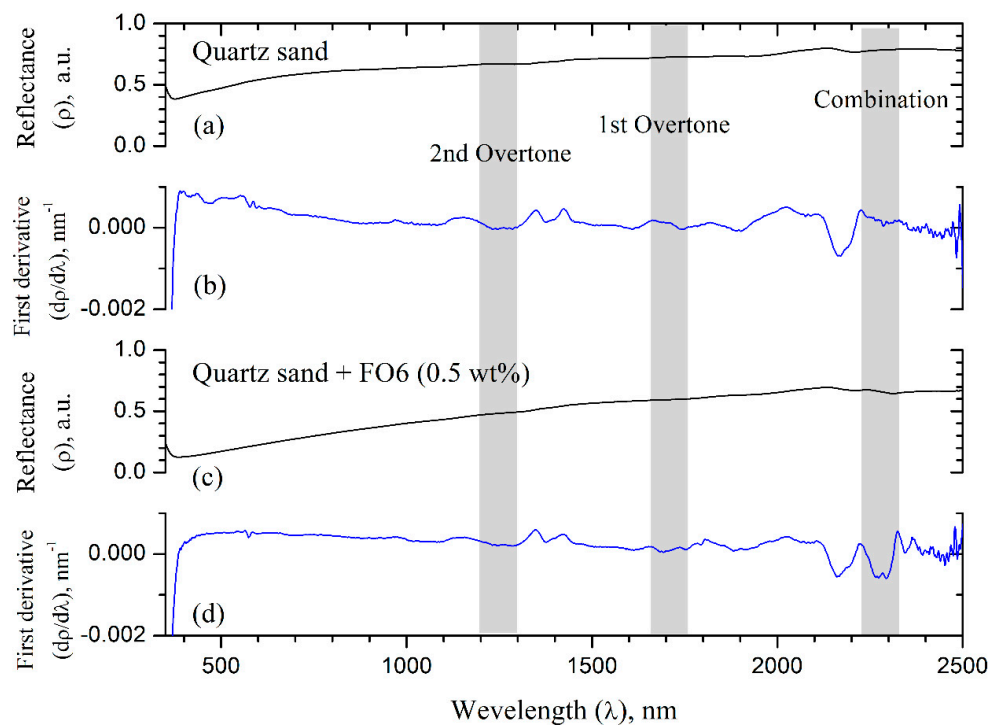


Figure 1. (a) Fuel oil 6 spectral signature of pristine quartz sand. (b) The first derivative of the diffuse reflectance spectra shown in (a). (c) Fuel oil spectral signature of quartz sand spike with 0.5 wt.% on gravimetry bases. (d) The first derivative of the diffuse reflectance spectra shown in (c).

3.2. Calibration Model

A visual inspection of the DR spectra in Figure 2 indicates that they are systematically affected by the amount of FO6. Although the broad bands resulting from C–H overtones hinder the quantitative interpretation of DR spectra, the DR spectra of QS and soil spiked with FO6 decreases in its global intensity as the FO6 concentration increases (Figure 2), as expected [16]. The three vertical bars highlight the petroleum 2nd and 1st overtone C–H stretch band (1700 nm) and the C–H stretch combination overtones band (2300 nm). Chakraborty et al. [10] reported that the 1st overtone of the C–H stretch band makes the most significant contribution for analysis of oil systems. However, our results suggest that the C–H stretch combination band is the one that makes the significant contribution for analysis of FO6 systems. Thus, we developed the *UHI* and later the FO6 concentration calibration model to quantify the *TPH* [20].

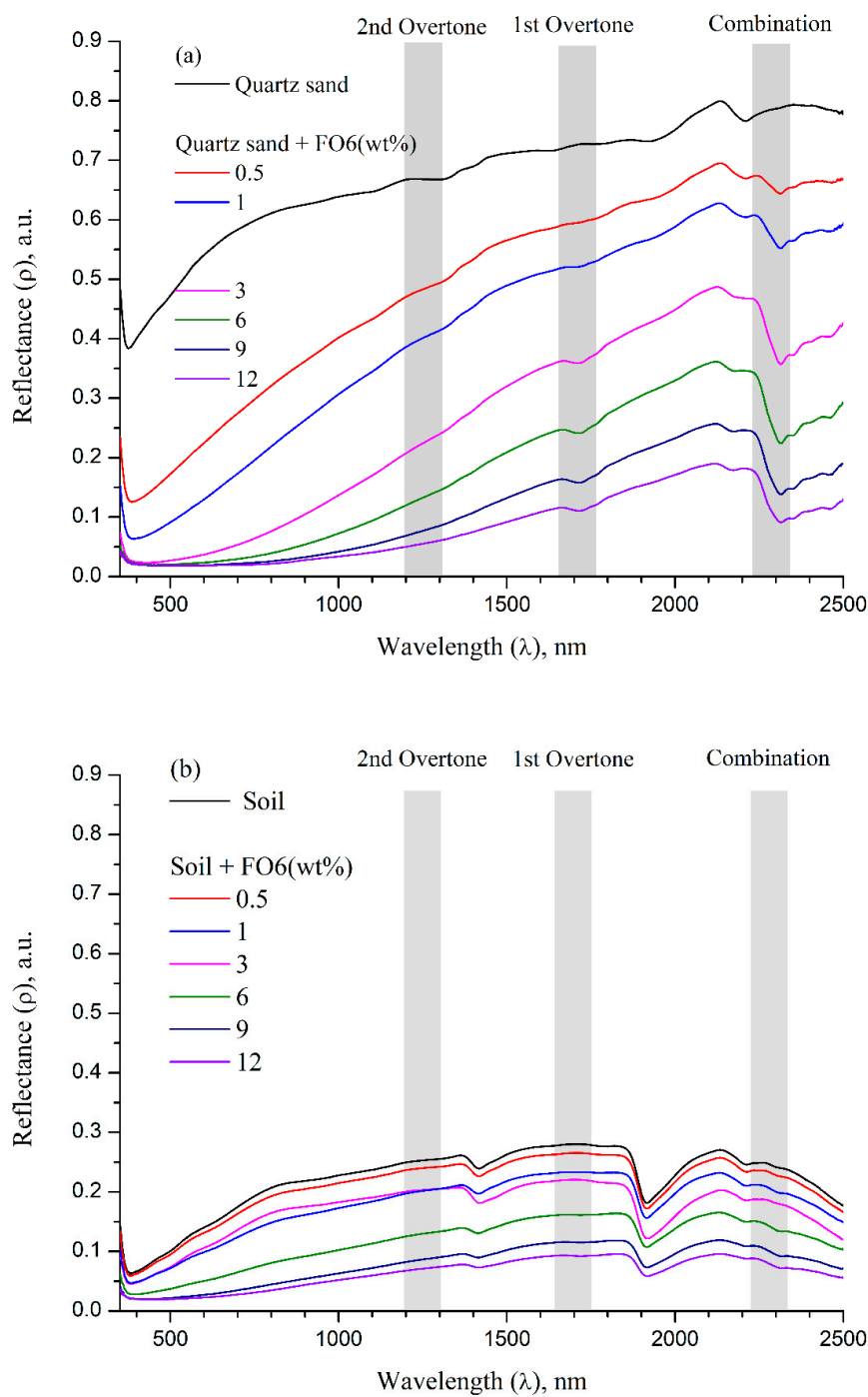


Figure 2. The diffuse reflectance spectra of (a) quartz sand and (b) soil samples spiked with fuel oil 6.

For the sake of clarity and the comparison purpose, the values of the Khun (*KHI*), NASA (*NHI*), and *UHI* are shown in Figure 3. *UHI* behavior is more intuitive than the other indices. The value of *UHI* increases as the FO6 concentration increases (Figure 3e,f), while the *KHI* (Figure 3a,b) works well at a lower concentration and collapses at a concentration bigger than 4 wt.% in QS samples and ultimately collapses in an SS. The *NHI* values decrease as the FO6 concentration increases, and it is more sensitive at a lower FO6 concentration (3 wt.%). However, its global magnitude decreases in SS.

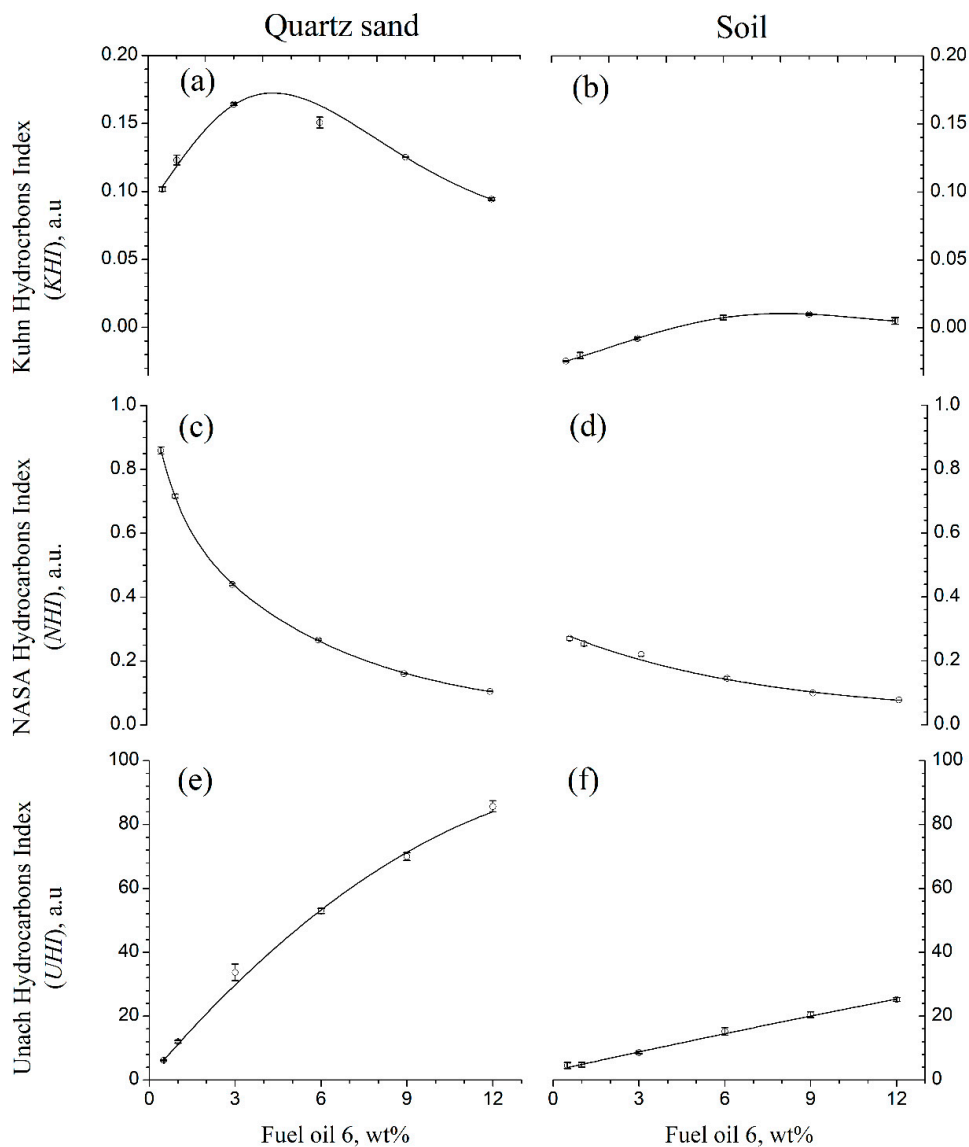


Figure 3. Hydrocarbon index values in quartz sand and soil samples spiked with fuel oil 6 at a concentration of 0.5, 1, 3, 6, 9, and 12 wt%. (a,b) Khun hydrocarbon index (KHI). (c,d) NASA index (NHI). (e,f) Unach index (UHI).

The calibration model for QS samples and SS shows an excellent agreement with experimental data $R^2 = 0.9989$ and $R^2 = 0.9968$, respectively (Figure 4). The SS calibration model suggests that other spectral features mask the FO6 features around 2300 nm, and the range of variation of the soil UHI decreases, and so does its sensibility. However, the calibration model shows good results in sandy soil. Cloutis [23] reported a similar result in medium-bitumen tar sand.

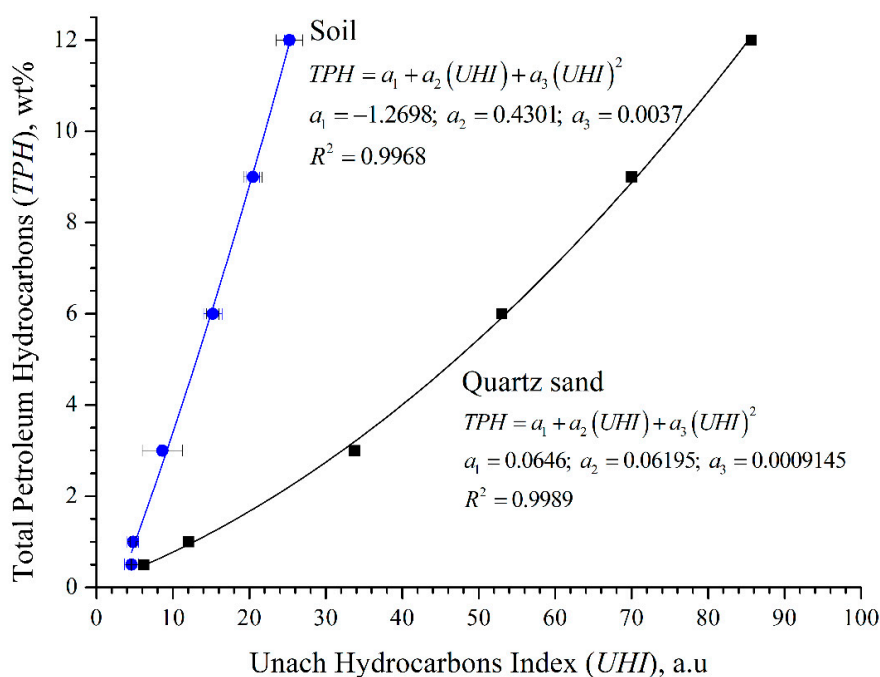


Figure 4. Calibration model using the Unach hydrocarbon index.

3.3. Assessing Bioremediation

The results suggest that the dominant mechanism in the degradation of FO6 was biodegradation, which was carried out by *P. aeruginosa*, since before its contamination with FO6, the samples were sterilized in an autoclave for 4 h and at 115 °C and later inoculated with *P. aeruginosa*. Thus, the global reflectance increased as more days passed after the inoculation and the bioremediation advance. The DR spectra of contaminated samples tend to be more similar to uncontaminated samples (Figure 5).

P. aeruginosa is one of the best degraders of crude oil, and it is the main degrader responsible for the bioremediation process. In this process, FO6 is a rich source of organic compounds that serve as nutrients for the growth and development of *P. aeruginosa*. Darsa and Thattheyus [6] reported that *P. aeruginosa* exhibits an excellent ability to degrade n-hexadecane (C₁₆H₃₄). Das and Chandran [25] reported that *P. aeruginosa* in its catabolic cycle produces a biosurfactant called rhamnolipid, an enzyme considered biosurfactant that allows it to take the carbon from the hydrocarbon. The biosurfactant acts as an emulsifying agent that decreases surface tension and forms micelles.

The average values of the hydrocarbon indices—UHI and TPH (Table 4)—decreased along the experimental period, suggesting that FO6 biodegradation by *Pseudomonas* in the QS sample and SS contaminated with FO6 decreased 13.6% and 45.8% in 23 days, respectively. While the QS samples showed the lower recovery rate (13.6%), the Entisols SS showed the higher recovery rate (45.8%). Our results suggested that *P. aeruginosa* did not survive in the QS samples, whereas it survives in SS. In the literature, it is accepted that temperature, pH, and availability of carbon nutrients such as N and P, among others, control the biodegradation process [25]. We did not measure any of this parameter because we were more interested in performing DR spectroscopy to assess the FO6 contaminated sample.

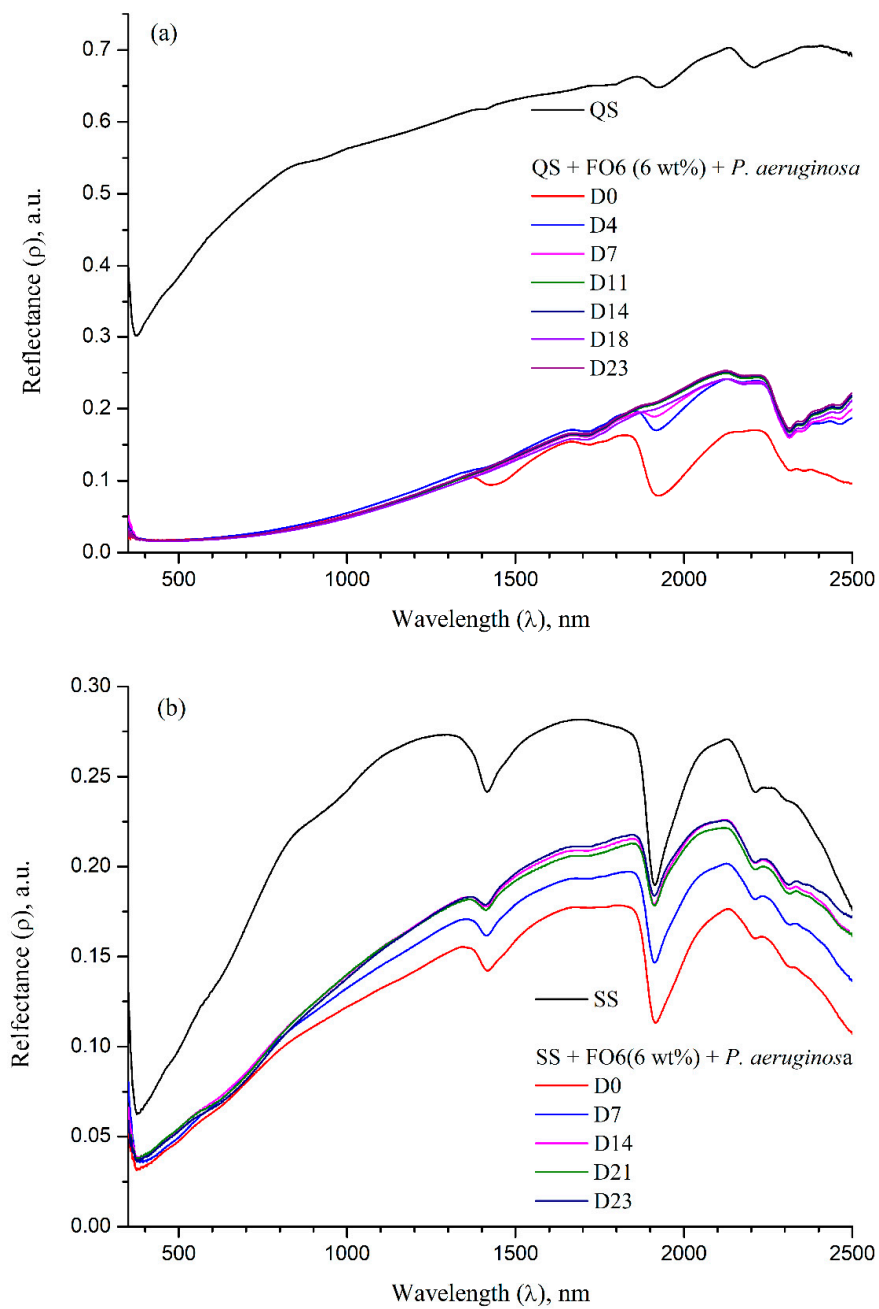


Figure 5. Diffuse reflectance spectra of Quartz sand (a) and soil samples (b) spiked with FO6 and inoculated with *Pseudomonas aeruginosa* on day 0 (D0). Diffuse reflectance spectra recorded on day 0 (D0), 4 (D4), 7 (D7), 11 (D11), 14 (D14), 21 (D21), and 23 (D23) after inoculation. At the bottom is the DR spectrum on D0 and at the top is the spectrum reflectance spectrum of pristine quartz sand (QS) and soil sample (SS).

Table 4. Hydrocarbon index (*UHI*) and total petroleum hydrocarbons (*TPH*) in samples spiked with fuel oil 6 on day 0 and going through a bioremediation process.

	Day 0	Day 7	Day 14	Day 21	Day 23
Mean Unach hydrocarbon index (<i>UHI</i>), a.u					
Quartz sand	48.464	48.224	45.324	43.946	43.433
Soil sample	13.221	10.516	9.614	9.200	8.476
Mean total petroleum hydrocarbons (<i>TPH</i>), wt.%					
Quartz sand	5.3137 (0.1076) * a	5.2784 (0.1685) * a	4.8551 (0.1735) * b	4.6586 (0.1437) * b	4.5863 (0.1408) * b
Soil sample	5068 (0.1860) * a	3.718 (0.4352) * b	3.281 (0.0506) * bc	3.085 (0.0454) * c	2745 (0.0319) * c

* Standard deviation in the parentheses. Means that do not share a letter are significantly different.

4. Conclusions

The use of DR spectroscopy and determination of the FO6 spectral signature allowed the assessment of the bioremediation process of QS and Entisols SS samples spiked with FO6 and inoculated with *P. aeruginosa*. The results showed that DR decreased with increasing the FO6 concentration, and soil properties affected the degree of biodegradation.

P. aeruginosa has shown to be highly effective as a bioremediation agent in the restoration of Entisols soil ecosystems contaminated with FO6. Thus, bioremediation with *P. aeruginosa* represents a viable technical solution for the disposal and remediation of Entisols soils contaminated with FO6, since the rate of recovery was 45.8% in 23 days.

The molasses inoculum was very convenient and practical for the bioaugmentation of *P. aeruginosa*. This bioaugmentation methodology showed great potential for the remediation of soils contaminated with FO6.

The *UHI* and the calibration model to quantify *TPH* have shown to be convenient for the assessment of the bioremediation process of sandy soil and Entisols soil. However, more studies are necessary to validate the use of the *UHI* and DR spectroscopy in other soils.

Author Contributions: C.O.M. and V.J.G. conceived and designed the experiments; A.R.C. and K.G.M. performed the experiment; C.O.M. and V.J.G. analyzed the data and contributed reagents/materials/analysis tools; C.O.M. and V.J.G. wrote the paper.

Funding: This research was funded by UNIVERSIDAD NACIONAL DE CHIMBORAZO, Riobamba Ecuador, through the project "Soil organic carbon and sequestration in Ecuadorian paramo ecosystem"

Acknowledgments: The authors express their gratitude to the Vice-Rectorate of Postgraduate Studies and Research of the National University of Chimborazo (Unach) through the group "Clean Energy and Environmental."

Conflicts of Interest: The authors declare no conflict of interest.

References

- Oudejans, L. *International Decontamination Research and Development Conference*; Report on the 2016 U.S. Environmental Protection Agency (EPA); EPA/600/R-17/174; EPA: Washington, DC, USA, 2017; p. 117.
- Yuniati, M.D. Bioremediation of petroleum-contaminated soil: A review. In *IOP Conference Series: Earth and Environmental Science*; IOP Publishing: Bristol, UK, 2018.
- Chen, M.; Xu, P.; Zeng, G.; Yang, C.; Huang, D.; Zhang, J. Bioremediation of soils contaminated with polycyclic aromatic hydrocarbons, petroleum, pesticides, chlorophenols and heavy metals by composting: Applications, microbes and future research needs. *Biotechnol. Adv.* **2015**, *33*, 745–755. [[CrossRef](#)] [[PubMed](#)]
- Zobell, C.E. Action of microorganisms on hydrocarbons. *Bacteriol. Rev.* **1946**, *10*, 1–49. [[PubMed](#)]

5. Andreoli, G.; Bulgarelli, B.; Hosgood, B.; Tarchi, D. *Hyperspectral Analysis of Oil and Oil-Impacted Soils for Remote Sensing Purposes*; European Commission Joint Research Centre: Luxembourg, 2007.
6. Darsa, K.V.; Thatheyus, A.J. Biodegradation of petroleum compound using pseudomonas aeruginosa. *Open Access Libr. J.* **2014**, *1*, 1–9. [[CrossRef](#)]
7. Englert, C.J.; Kenzie, E.J.; Dragun, J. Bioremediation of petroleum products in soil. In *Practices for Petroleum Contaminated Soils*; Calabrese, E.J., Kostecki, P.T., Eds.; Lewis Publishers: Chelsea, MI, USA, 1993; pp. 11–130.
8. López De Mesa, J.B.; Quintero, G.; Vizcaíno Guevara, A.L.; Cáceres, D.C.J.; Riaño, S.M.G.; García, J.M. Bioremediación de suelos contaminados con hidrocarburos derivados del petróleo. *Nova* **2006**, *4*, 82–90. [[CrossRef](#)]
9. Scafutto, R.D.M.; de Souza Filho, C.R. Quantitative characterization of crude oils and fuels in mineral substrates using reflectance spectroscopy: Implications for remote sensing. *Int. J. Appl. Earth Obs. Geoinf.* **2016**, *50*, 221–242. [[CrossRef](#)]
10. Chakraborty, S.; Weindorf, D.C.; Zhu, Y.; Li, B.; Morgan, C.L.S.; Ge, Y.; Galbraith, J. Spectral reflectance variability from soil physicochemical properties in oil contaminated soils. *Geoderma* **2012**, *177–178*, 80–89. [[CrossRef](#)]
11. Douglas, R.K.; Nawar, S.; Alamar, M.C.; Mouazenab, A.M.; Coulona, F. Rapid prediction of total petroleum hydrocarbons concentration in contaminated soil using vis-NIR spectroscopy and regression techniques. *Sci. Total Environ.* **2018**, *616–617*, 147–155. [[CrossRef](#)] [[PubMed](#)]
12. Okparanma, R.N.; Coulon, F.; Mouazen, A.M. Analysis of petroleum-contaminated soils by DRspectroscopy and sequential ultrasonic solvent extraction-gas chromatography. *Environ. Pollut.* **2014**, *184*, 298–305. [[CrossRef](#)] [[PubMed](#)]
13. Okparanma, R.N.; Coulon, F.; Mayr, T.; Mouazen, A.M. Mapping polycyclic aromatic hydrocarbon and total toxicity equivalent soil concentrations by visible and near-infrared spectroscopy. *Environ. Pollut.* **2014**, *192*, 162–170. [[CrossRef](#)] [[PubMed](#)]
14. Douglas, R.K.; Nawar, S.; Cipullo, S.; Alamar, M.C.; Coulon, F.; Mouazen, A.M. Evaluation of vis-NIR reflectance spectroscopy sensitivity to weathering for enhanced assessment of oil contaminated soils. *Sci. Total Environ.* **2018**, *626*, 1108–1120. [[CrossRef](#)] [[PubMed](#)]
15. Schwartz, G.; Ben-Dor, E.; Eshel, G. Quantitative assessment of hydrocarbon contamination in soil using reflectance spectroscopy: A ‘multipath’ approach. *Appl. Spectrosc.* **2013**, *67*, 1323–1331. [[CrossRef](#)] [[PubMed](#)]
16. Hörig, B.; Kühn, F.; Oschütz, F.; Lehmann, F. HyMap hyperspectral remote sensing to detect hydrocarbons. *Int. J. Remote Sens.* **2001**, *22*, 1413–1422. [[CrossRef](#)]
17. Kühn, F.; Oppermann, K.; Hörig, B. Hydrocarbon index-An algorithm for hyperspectral detection of hydrocarbons. *Int. J. Remote Sens.* **2004**, *25*, 2467–2473. [[CrossRef](#)]
18. Smejkalová, E.; Bujok, P.; Píkl, M. Study of old ecological hazards, oil seeps and contaminations using earth observation methods-Spectral library for oil seep. *Arch. Environ. Prot.* **2017**, *43*, 3–10. [[CrossRef](#)]
19. Short, N. *Finding Oil and Gas in Oklahoma, the Remote Sensing Tutorial (An Online Handbook)*; Code 935; Goddard Space Flight Center, NASA: Greenbelt, MD, USA, 1998.
20. Garcia, V.J.; Marquez, C.O.; Cedeño, A. *Método y sistema para la detección y evaluación rápida de hidrocarburos en suelos*; IEPI-2018-1179; IEPI: Quito, Ecuador, 2018.
21. Termoesmeraldas. *Reporte interno de la Central Térmica Termoesmeraldas*; Termoesmeraldas: Esmeraldas, Ecuador, 2014; p. 25.
22. Todd, G.D.; Chessin, R.L.; Colman, J. *Toxicological Profile for Total Petroleum Hydrocarbons (TPH)*; Agency for Toxic Substances and Disease Registry: Atlanta, GA, USA, 1999; p. 315. [[CrossRef](#)]
23. Cloutis, E.A. Spectral reflectance properties of hydrocarbons: Remote-sensing implications. *Science* **1989**, *245*, 165–168.
24. Asadzadeh, S.; de Souza Filho, C.R. Spectral remote sensing for onshore seepage characterization: A critical overview. *Earth-Sci. Rev.* **2017**, *168*, 48–72. [[CrossRef](#)]
25. Das, N.; Chandran, P. Microbial degradation of petroleum hydrocarbon contaminants: An overview. *Biotechnol. Res. Int.* **2011**, *2011*, 1–13. [[CrossRef](#)] [[PubMed](#)]

